



DESIGN OPTIMIZATION OF A SUBMERGED VANE WITH STREAMLINED PROFILE FOR SEDIMENT MANAGEMENT IN RIVERS

Huei-Tau Ouyang

Department of Civil and Environmental Engineering, National Ilan University, Yilan County, Taiwan, R.O.C,
htouyang@niu.edu.tw

Jihn-Sung Lai

Hydrotech Research Institute, National Taiwan University, Taipei, Taiwan, R.O.C.

Follow this and additional works at: <https://jmstt.ntou.edu.tw/journal>



Part of the [Engineering Commons](#)

Recommended Citation

Ouyang, Huei-Tau and Lai, Jihn-Sung (2013) "DESIGN OPTIMIZATION OF A SUBMERGED VANE WITH STREAMLINED PROFILE FOR SEDIMENT MANAGEMENT IN RIVERS," *Journal of Marine Science and Technology*: Vol. 21: Iss. 3, Article 11.

DOI: 10.6119/JMST-012-0606-1

Available at: <https://jmstt.ntou.edu.tw/journal/vol21/iss3/11>

This Research Article is brought to you for free and open access by Journal of Marine Science and Technology. It has been accepted for inclusion in Journal of Marine Science and Technology by an authorized editor of Journal of Marine Science and Technology.

DESIGN OPTIMIZATION OF A SUBMERGED VANE WITH STREAMLINED PROFILE FOR SEDIMENT MANAGEMENT IN RIVERS

Huei-Tau Ouyang¹ and Jihn-Sung Lai²

Key words: submerged vane, genetic algorithm, shape optimization, NACA, Bezier spline.

ABSTRACT

The design of the submerged vane, a flow training structure for sediment management in rivers, is optimized using a Genetic Algorithm. The vane considered in this study has a foil-like sectional profile and a tapered outline. The sectional profile of the vane is based on two types of shape formulations: (1) NACA's four-digit wing profiles, and (2) profiles comprising two Bezier splines. By using Elitist and Crowding factor models, the optimization proceeds by creating successively improved generations of vanes. The final design for the vane with NACA profile has higher lift yet larger drag. Conversely, the final design for the vane with B-spline profile generates lower lift but also smaller drag.

I. INTRODUCTION

Submerged vanes are small flow training structures installed on the streambed to modify the near-bed flow pattern and redistribute flow and sediment transport. The vanes function by generating secondary circulation in the flow. The circulation alters magnitude and direction of the bed shear stresses and causes a change in the distributions of velocity, depth, and sediment transport in the area affected by the vanes. As a result, the riverbed aggrades in one portion of the channel cross-section and degrades in another. Vanes have been used successfully for protection of stream banks against erosion and amelioration of shoaling problems at water intakes and bridge crossings.

As an example, the vanes have been used extensively to stop or reduce erosion in river curves. In such an application,

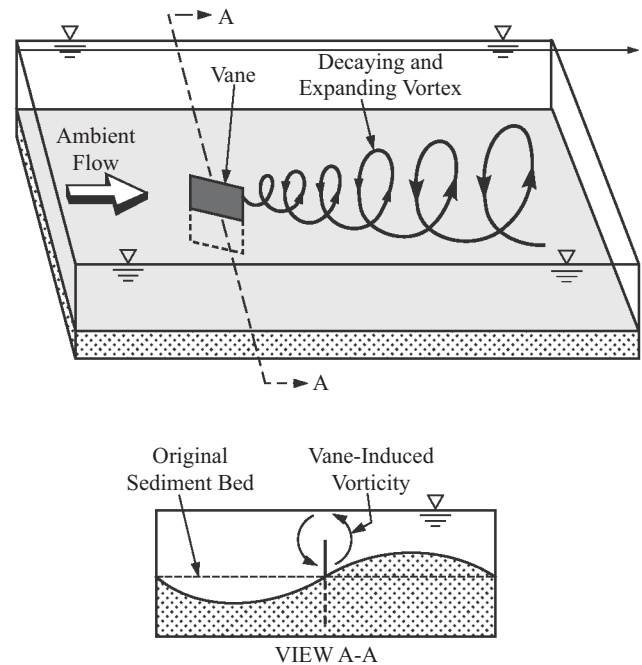


Fig. 1. Submerged vane and vane-induced vortex.

the vanes are laid out so that the vane-generated secondary current eliminates the centrifugally induced secondary current, which is the root cause of bank undermining. The centrifugally induced secondary current in river bends, also known as the transverse circulation or helical motion, results from the difference in centrifugal acceleration along a vertical line in the flow because of the nonuniform vertical profile of the velocity. The secondary current forces high-velocity surface current outward and low-velocity near-bed current inward. The increase in velocity at the outer bank increases the erosive attack on the bank, causing it to fail. By directing the near-bed current toward the outer bank, the submerged vanes counter the centrifugally induced secondary current and, thereby, inhibit bank erosion. Fig. 1 gives an illustration for the submerged vane and the vane-induced vortex.

So far, the vanes have been either flat plates (in most cases) or slightly curved foils with a twist toward the tail end [10-12].

Paper submitted 10/06/10; revised 04/24/12; accepted 06/06/12. Author for correspondence: Huei-Tau Ouyang (e-mail: htouyang@niu.edu.tw).

¹ Department of Civil and Environmental Engineering, National Ilan University, Yilan County, Taiwan, R.O.C.

² Hydrotech Research Institute, National Taiwan University, Taipei, Taiwan, R.O.C.

The design of the latter has been based mainly on engineering intuition without rigorous optimization. This study is an effort to use advanced optimization techniques to refine the design and improve efficiency. Since many vanes are often required in any given project, an improved vane design will cut back on the number of vanes required and thus reduce construction cost.

This paper summarizes the design process. Following a formal definition of the optimization problem, the paper describes the method for calculating the flow around the vane, the features of the genetic algorithm, the design procedure, and results, including the evolution history of the vane shapes.

II. FORMULATION OF THE DESIGN OPTIMIZATION PROBLEM

The optimization problem is formulated following the standard three-step procedure suggested by Arora [2] as follows: (1) Identification and definition of design variables, (2) Identification and definition of objective function, and (3) Identification and definition of constraints. Each step is detailed in the following.

1. Identification and Definition of Design Variables

As illustrated in Fig. 2, the general shape of the vane investigated in this study has a trapezoidal outline with foil-like cross-section. The coordinate system is as shown in the figure. The origin is located at the base of the leading edge of the vane. The x coordinate is following the direction from the leading edge to the trailing edge of the vane; the z coordinate is in the vertical direction and positive upward; the y direction is perpendicular to the other two directions following the left-hand rule.

Since the vane is tapering off along the vertical direction, the distance between the leading edge and the trailing edge of the vane (namely the ‘chord’ following Wing Theorem) is gradually becoming shorter from the base section to the top section. For simplicity, the cross-sectional shape for each of the vane-sections remains the same with the size scaling down linearly from the base to the top of the vane. Also, the vane is unswept with its quarter-chord line being a straight vertical line, as depicted in Fig. 2. The shape of the vane thus defined has a trapezoidal silhouette controlled only by one design variable λ defined as the ratio of the top-chord to the base-chord, i.e. $\lambda = L_t/L_b$, and has the same profiles at each cross-section with their sizes linearly scaling down from the base to the top by the taper-ratio λ as well.

Two types of vanes with different vane-section formulations are studied. In the first one, the four-digit airfoil family of NACA (National Advisory Committee for Aeronautics) is adopted as the vane-section. In the second one, the vane-section is decomposed into two Bezier splines dissected at the leading edge and the trailing edge of the vane. Herein, the first type of vanes will be named the NACA vane and the second type the B-spline vane.

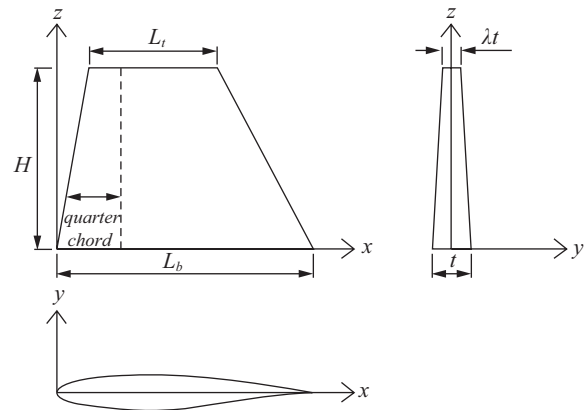


Fig. 2. Definition sketch of a vane with streamlined profile.

The NACA sectional profile consists of two components: (1) the mean line, which is the centerline in-between the two surfaces of the cross-section dissected at the leading edge and the trailing edge, and (2) the thickness distribution of the cross-section along the mean line. The mean line and thickness distribution are defined by the following Eqs. [6]

Mean line:

$$y_c = \frac{m}{p^2}(2px - x^2), \quad x \leq p$$

$$y_c = \frac{m}{(1-p)^2}[(1-2p) + 2px - x^2], \quad x > p \quad (1)$$

Thickness distribution:

$$y_c = \pm \frac{t}{0.20}(0.29690\sqrt{x} - 0.12600x - 0.35160x^2 + 0.28430x^3 - 0.10150x^4) \quad (2)$$

where x = distance from the leading edge; m = maximum ordinate of mean line; p = position of maximum ordinate; t = maximum thickness.

The two surfaces of the NACA profile dissected by the leading edge and the trailing edge are generated by adding and subtracting the thickness distribution to the mean line in the normal direction, respectively, as illustrated in Fig. 3. Together with the taper ratio that defines the outline of the vane, 4 design variables are identified for constructing the shape of a NACA vane, namely m , p , t , and λ .

For the B-spline vane, two 3rd order B-splines each consists of 7 vertex points are utilized to generate the two surfaces of the sectional profile, as depicted in Fig. 4. Each vertex is designated by its x and y coordinates. The first and the last vertices of each B-spline are fixed at the leading edge and the trailing edge of the vane-section, respectively. To ensure a streamline profile with a smooth head for the vane-section,

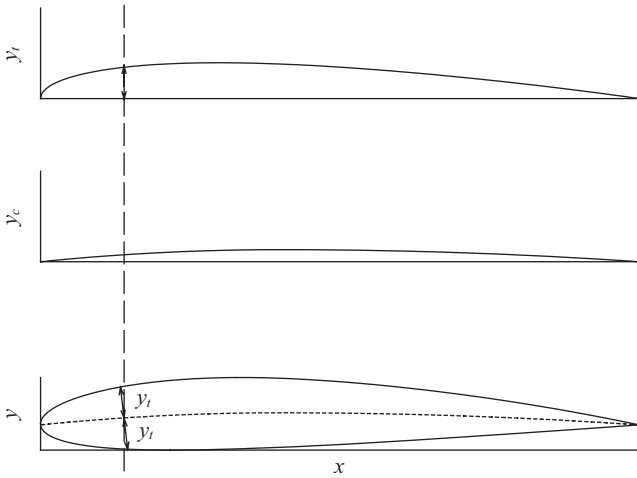


Fig. 3. Construction of a NACA profile.

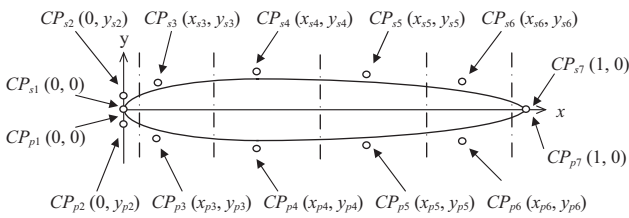


Fig. 4. Control points and design variables of a B-spline profile.

the x coordinate of the second vertex is set as the same as the leading edge while the y coordinate moving freely. The other vertices are free to move in both x and y direction within certain ranges. As depicted in Fig. 4, the design variables shaping the sectional profile of a B-spline vane are thus x_{s3} , x_{s4} , x_{s5} , x_{s6} , x_{p3} , x_{p4} , x_{p5} , x_{p6} , y_{s2} , y_{s3} , y_{s4} , y_{s5} , y_{s6} , y_{p2} , y_{p3} , y_{p4} , y_{p5} , and y_{p6} . Together with the taper ratio λ , totally 19 design variables are identified for charactering the shape of a B-spline vane.

The dimension of a vane are characterized by two parameters: (1) the ratio of vane-height to vane-length at the base, H/L_r ; and (2) the ratio of vane-height to water-depth, H/d . Ouyang [11] have shown that the efficiency of a vane increases with increasing H/L_r . However, it has also been shown that a vane with H/L_r higher than 0.45 tends to suffer structure instability and is therefore not feasible from practical considerations [7]. Therefore, the height-to-length ratio H/L_r is determined as the upper limit as 0.45 in this study and is not considered as a design variable for the shape optimization problem. For H/d , it has also been found by Odgaard and Mosconi [8] that the area of the streambed affected by the vane reaches maximum when $H/d = 0.5$. To maximize the affected area of the vane, H/d is fixed at 0.5 in this study and is also not considered as a design variable.

2. Identification and Definition of Objective Function

Previous researchers [7, 9, 10] have shown that the number

of vanes required to eliminate the secondary current in a river bend is

$$N = \frac{2}{C_L} \frac{r\phi b}{LH} \frac{d}{r} G \quad (3)$$

where N = number of vanes, L = vane length, H = vane height, r = bend radius of curvature, ϕ = bend angle, b = channel width, C_L = vane lift coefficient, and G is the vane factor which is a function of the power-law velocity profile exponent n and H/d .

Eq. (3) indicates that the number of vanes required in a vane system is inversely proportional to the vane-induced lift. If each vane can generate stronger lift force, the number of vanes can be reduced.

On the other hand, it is inevitable for a vane system to produce drag in the flow which increases the channel resistance and change the energy slope of the channel. The vane-induced change in energy slope has been estimated by Odgaard and Mosconi [8] to be

$$\Delta S_f = \frac{NF_D - \Delta M}{r\phi b \rho g d} \quad (4)$$

where ΔS_f = vane-induced energy slope change; F_D = vane-induced drag; and ΔM = vane-induced difference in momentum flux between the upstream and downstream end of the reach.

Eq. (4) indicates that the change in the channel's energy slope relates to the total drag induced by the vane system. To minimize the influence of a vane system on the overall channel characteristics, the induced change in energy slope should be as small as possible.

Based on the aforementioned arguments, two design goals are concluded: (1) Max. C_L ; and (2) min. C_D . To avoid premature domination for one design objective over the other one during the optimization process, the changes of the two objectives must be of the same order. Following the suggestion of Jameson [5], the objective function is defined by combining the two design goals as follows:

$$\text{Max. } f(\underline{X}) = \frac{C_L^2}{C_D} \quad (5)$$

3. Identification and Definition of Constraints

To avoid producing unreasonable vane-shapes, each of the design variables must be confined in a certain range. Table 1 gives the upper and lower bounds of the design variables for the NACA vanes based on the NACA data [1].

For the B-spline vanes, each vertex defining the cross-sectional profile is free to move within a certain range. Table 2 shows the upper and lower bounds for the x and y coordinates of each vertex by referring to the NACA foils.

Table 1. Upper and lower limits of the design variables for the NACA vanes.

Design variables	Lower limit	Upper limit
m	0.00	0.09
P	0.20	0.70
t	0.06	0.24
λ	0.10	1.00

Table 2. Upper and lower limits of the design variables for the B-spline vanes.

Design variables	Lower limit	Upper limit	Design variables	Lower limit	Upper limit
y_{s1}	0.00	0.21	x_{s2}	0.02447	0.20611
y_{s2}	0.00	0.21	x_{s3}	0.20611	0.50000
y_{s3}	0.00	0.21	x_{s4}	0.50000	0.79389
y_{s4}	0.00	0.21	x_{s5}	0.79389	0.97553
y_{s5}	0.00	0.21	x_{p2}	0.02447	0.20611
y_{p1}	-0.12	0.00	x_{p3}	0.20611	0.50000
y_{p2}	-0.12	0.06	x_{p4}	0.50000	0.79389
y_{p3}	-0.12	0.06	x_{p5}	0.79389	0.97553
y_{p4}	-0.12	0.06	λ	0.10	1.00
y_{p5}	-0.12	0.06			

III. GENETIC ALGORITHM

The objective function defined in Eq. (5) could be discontinuous due to sudden flow separation from the surface of the vane. A Genetic Algorithm (GA) is adopted in the study as an optimization tool due to its ability to cope with this type of objective functions.

In the GA, the shape of a vane is represented by a binary string named chromosome. A number of chromosomes were first generated randomly at the beginning and then evolved generations by generations following the procedure of selection, crossover and mutation in standard GA. To evaluate the performance of the vanes in a population, the binary string chromosome of each vane is first decoded back to the vane's physical shape. Following the computation of the flow field around the vanes, the performance for each of the vanes is then evaluated by Eq. (5).

A chromosome comprises a number of binary segments. Each binary segment is converted to an integer J_k by the following Eq.:

$$J_k = \sum_{j=1}^{N_{bit}} \delta_j^{(k)} 2^{N_{bit}-j+1}, \quad k=1, \quad N_{dv} \quad (6)$$

where N_{dv} is the number of design variables; N_{bit} is the digit of binary segments; $\delta_j^{(k)}$ (which is either 0 or 1) represents the

j^{th} position of the k^{th} binary segment. The range of J_k is thus $0 \leq J_k \leq 2^{N_{bit}} - 1$.

A mapping from the integer interval $[0, 2^{N_{bit}} - 1]$ of J_k to the real number interval $[f_{\min}, f_{\max}]$ for each of the design variables is constructed by the following Eq.

$$a_k = f_{\min}^{(k)} + \left[\frac{J_k}{2^{N_{bit}} - 1} \right] (f_{\max}^{(k)} - f_{\min}^{(k)}), \quad k=1, \quad N_{dv} \quad (7)$$

where $f_{\min}^{(k)}$ and $f_{\max}^{(k)}$ are the lower and upper bounds for each design variable, as given in Table 1 and 2 for NACA vane and B-spline vane, respectively.

Since the design variables are represented by binary chromosomes in GA, the decoded values of these design variables are therefore discrete and the preferred precision has to be decided. By referring to NACA data (Table 1), the precision for each design variable is set as 0.0001 in this study. The length of a binary chromosome for a NACA vane is thus 48 and the search space is $2^{48} \approx 2.81 \times 10^{14}$. For a B-spline vane, the chromosome length is 226 and the search space is $2^{226} \approx 1.08 \times 10^{68}$.

In the selection phase, the vanes are chosen based on their fitness (performance) by the linear scaling method and the simple biased roulette wheel method [4]. To prevent premature convergence, the elitist model proposed by De Jong [3] is also utilized in the selection phase. The elitist model enforces preserving the chromosomes that have shown the best performance. In the elitist model, the vanes are classified into three groups according to their scaled fitness: Group 1. A specific number of vanes that have the highest fitness; Group 2. Same number of vanes as in group 1 yet have worse (not necessarily the worst) fitness; Group 3. The remaining vanes that are not included in group 1 and 2.

The chromosomes of the vanes in group 1 are preserved directly into the next generation while the chromosomes in group 2 die out without any contribution to the next generation. The remaining population in the next generation is then produced from the gene pool comprising the chromosomes in group 1 and 3 only.

De Jong's [3] crowding factor model which permit less survival pressure for the elitist to achieve higher production rate is also adopted in present study. Each time a new chromosome is generated, the crowding factor model replaces the old chromosome that is most similar to the new one. The improvement on convergence rate of this model has been observed in many studies [4].

IV. FLOW SOLVER

A flow solver based on the lifting panel method is adopted to evaluate the performance of the vanes. The lifting panel method simulates the flow field by a vortex ring system clothing the surface of a vane with initially unknown strength. The velocity at an arbitrary point induced by the vortex-ring system is obtained by the Biot-Savart law [11]

$$\bar{q}_j = \sum_{i=1}^k \frac{\Gamma_i}{4\pi} \sum_{s=1}^4 \frac{\bar{r}_{is1} \times \bar{r}_{is2}}{|\bar{r}_{is1} \times \bar{r}_{is2}|^2} \bar{r}_{is0} \cdot \left(\frac{\bar{r}_{is1}}{|\bar{r}_{is1}|} - \frac{\bar{r}_{is2}}{|\bar{r}_{is2}|} \right) \quad (8)$$

where \bar{q}_j is velocity vector, k is the number of the vortex rings, Γ_i is the strength for each vortex ring; \bar{r}_{is0} is the position vector of each vortex segment, \bar{r}_{is1} and \bar{r}_{is2} are the vectors from the target point to each end of the vortex segment.

The strength of each vortex ring is then determined by applying a Dirichlet boundary condition of zero normal velocity at the vane surface. To account for the boundary effects of water surface and riverbed, the method of image [11-13] is utilized in the flow field calculation. The effect of the bottom boundary is modeled using an image of the vane relative to the bottom. The vane and its image thus comprise a wing inclined with the approaching flow. For flow with the Froude number less than unity, the free surface of the flow can be taken as a rigid boundary [13]. The effect of the free surface boundary is modeled using an image of the wing with respect to the free surface, and an image of this image with respect to the bottom boundary. Theoretically, the two boundaries will produce an infinite number of images of the vane. However, the effect of the images diminishes as the distance between the images and the real vane increases. Numerical tests show that the increment of lift and drag coefficients drops to about 1% or less when 4 images or more are used.

V. DESIGN PROCEDURE

Following the Genetic Algorithm, the procedure of searching for the optimal vane becomes an evolution process. The vanes evolve and gradually improve their performance generations by generations. The procedure is as follows:

- Step 1. The chromosomes of the first generation of vanes are generated randomly.
- Step 2. The real values of the design variables for the vanes are recovered by decoding the chromosomes.
- Step 3. The shape of each vane is reconstructed following the procedure described in section 2.1.
- Step 4. The flow field corresponding to each vane is computed by the flow solver. The performance of each vane is then evaluated according to the objective function based on the flow field calculation.
- Step 5. The chromosomes for the next generation of vanes are produced by the GA following the procedure described in previous section.
- Step 6. Repeat step 2 to 5 until the stop criterion is reached.

VI. RESULTS

The aforementioned design procedure for a vane is tested under the typical river flow condition with 3 m of water depth and 1 m/s of flow velocity. The population consists of 100

Table 3. CPU time for GA runs (in seconds).

Run No.	NACA vane	B-spline vane
1	148952.4783	482764.0262
2	135897.8864	452077.2916
3	155503.5070	426615.3010
4	152506.5951	412515.2759
5	137994.2325	505213.2555
6	120070.6760	376415.4917
7	125522.8106	503121.3860
8	126951.5588	361444.8393
9	115670.9028	498150.5013
10	134932.1209	506371.4812

vanes in each generation. The evolution proceeds until the objective value remains unchanged for over 100 generations. 10 GA runs were performed and the best results are presented in the following. The calculations were performed on a Intel Core i7 3.07 GHz computer and the CPU time for each GA run is listed in Table 3.

1. Vanes with NACA Profile

The 3D view of the optimal NACA vane obtained by GA is presented in Fig. 5. The associated sectional profile and the silhouette of the vane are shown in Fig. 6 and Fig. 7, respectively. For comparison, the initial shape is also shown in the figures. As seen in Fig. 6, the sectional profile of the optimal vane is not as camber as the initial profile, suggesting that the lift induced by the final vane might be smaller than that of the initial vane. However, it is also seen in Fig. 7 that the silhouette of the final vane is much tapered than that of the initial vane. It has been proved in wing theorem that a vane with tapered outline has lower drag. The objective values for the final vane is 5.0048 and for the initial vane is 2.2730. The overall performance of the final vane is much higher than the initial vane.

Fig. 8 gives the evolution history of the lift and drag coefficients for the optimal vane in each generation. As the figure shows, the fluctuation of both the lift and drag coefficients indicates the competition between the two design goals. This is a desirable feature because it signifies that the search direction is not dominated by either one design goal only.

It is also seen in the figure that the lift and drag coefficients of the vanes were generally decreasing along the evolution. The lift coefficient C_L declines from 0.1911 for the initial vane to 0.1538 for the final vane. The reason for this might be due to the less camber profile of the final vane, as shows in Fig. 6. The declination for the drag coefficient C_D is even more evident, starting from 0.0161 for the initial vane to 0.0047 for the final vane. This might be due to the much tapered outline of the final vane, as seen in Fig. 7.

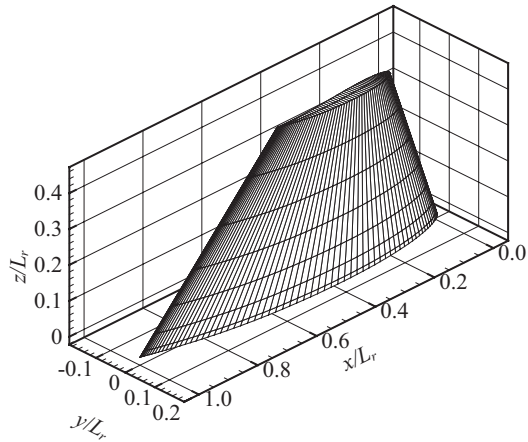


Fig. 5. Optimal NACA vane ($d = 3$ m, $u = 1$ m/s).

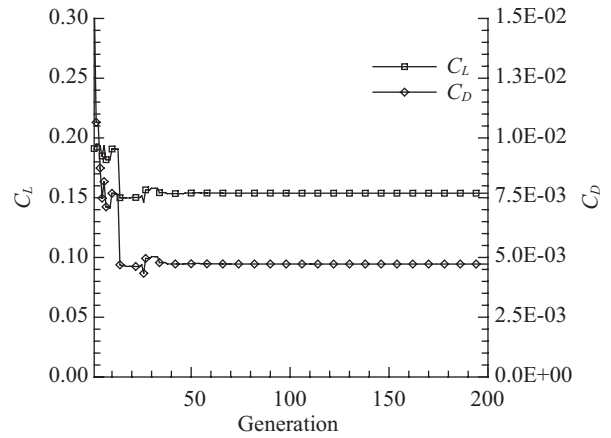


Fig. 8. Evolution of the lift and drag coefficients of the NACA vanes.

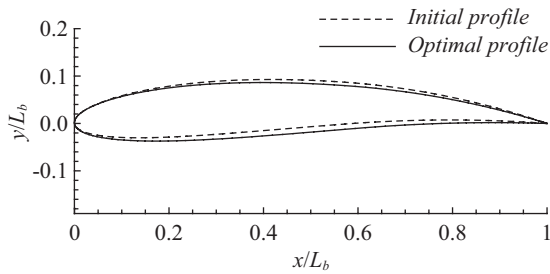


Fig. 6. The optimal and initial profiles of the NACA vanes.

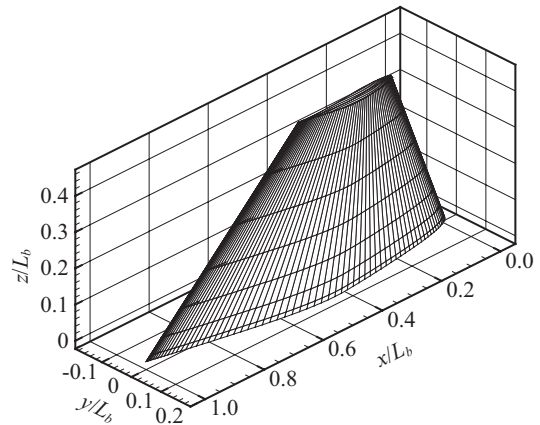


Fig. 9. Optimal B-spline vane ($d = 3$ m, $u = 1$ m/s).

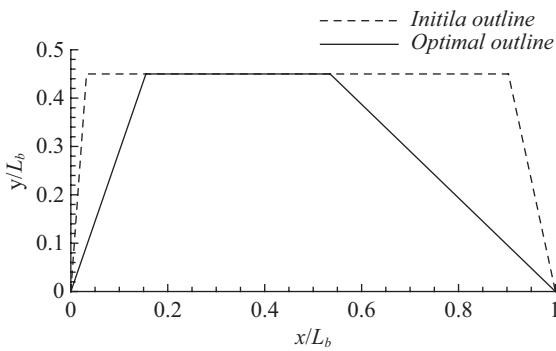


Fig. 7. The optimal and initial outlines of the NACA vanes.

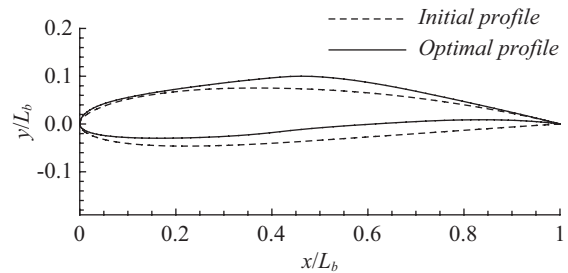


Fig. 10. The optimal and initial profiles of the B-spline vanes.

2. Vanes with B-spline Profile

For the B-spline vanes, the 3D view for the final shape obtained by GA is shown in Fig. 9. Figs. 10 and 11 are the associated sectional profile and the silhouette of the optimal vane, respectively. As seen in Fig. 10, the profile of the optimal vane is much camber than that of the initial vane, suggesting a higher lift of the optimal vane. Also, as observed in Fig. 11, the outline of the optimal vane is much taper than the initial one, suggesting a smaller drag of the optimal vane.

The evolution of the lift and drag coefficients of the B-spline vane is shown in Fig. 12. The lift coefficient C_L increases from 0.0864 for the initial vane to 0.1536 for the optimal vane, while the drag coefficient C_D declines from 0.0061 to 0.0042. The overall performance has improved

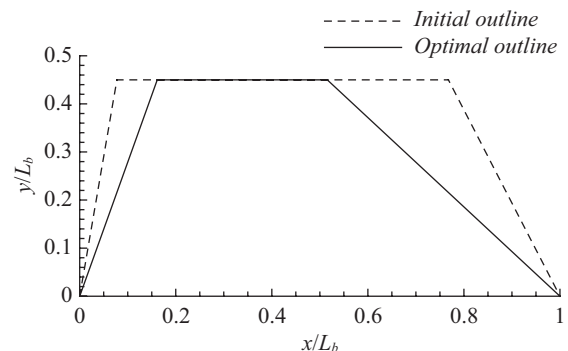


Fig. 11. The optimal and initial outlines of the B-spline vanes.

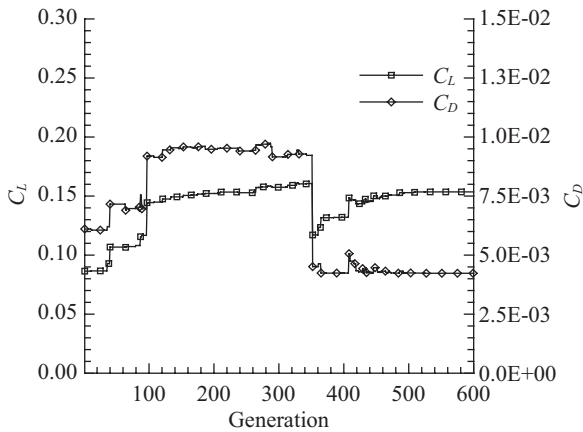


Fig. 12. Evolution of the lift and drag coefficients of the B-spline vanes.

from 1.2235 to 5.5689. The competition between the two design goals is clearly seen in the figure. Several major leaps are also seen in the figure signifying that the search might be jumping from one local optimum to the other ones, which is an advantageous feature of the GA permitting its capability on searching for the global optimum.

3. Comparison of the Results

Figs. 13 and 14 show the comparison of the sectional profiles and the silhouettes of the optimal NACA vane and the optimal B-spline vane, respectively. It appears that the final shapes of the two types of vanes are different. The associated C_L , C_D , and objectives of both vanes are listed in Table 4. For comparison, experimental data of some conventional NACA profiles are also listed in the table [1]. As the table shows, although the lift coefficients of the optimal NACA vane and the optimal B-spline vane are not higher than some of the conventional NACA profiles, the drag coefficients of the optimal vanes are lower than all of the conventional NACA profiles. As a result, the objective values of the optimal vanes are higher than that of the conventional NACA profiles. Comparison of the optimal NACA vane and the optimal B-spline vane shows that the lift induced by the optimal NACA vane is a little higher than that of the B-spline vane. The difference is about 0.13%. In contrast, the drag of the optimal NACA vane is higher than that of the B-spline vane with a difference of about 10.6%, which is much higher than the difference in C_L . Comparing the objective values of the two types of vanes, the overall performance of the optimal B-spline vane is about 11.3% higher than that of the optimal NACA vane. Despite of the different profiles of the two optimal vanes, the lift and drag coefficients for the two vanes are similar to each other. Observing the two profiles shown in Fig. 13, it is seen that the vertex on the upper surface of the optimal B-spline vane is a little closer to the trailing edge than that of the NACA vane, which delays the emerge of the positive pressure gradient near the trailing edge. As a result, the drag force on the B-spline vane is lower

Table 4. Comparison of the vanes.

Vane type	C_L	C_D	Objective
Opt. NACA vane	0.1538	0.0047	5.0048
Opt. B-spl vane	0.1536	0.0042	5.5689
NACA 1408	0.0976	0.0052	1.8315
NACA 1410	0.1071	0.0052	2.2053
NACA 1412	0.1446	0.0058	3.6055
NACA 2415	0.1776	0.0068	5.0047
NACA 2421	0.1259	0.0070	2.2659
NACA 2424	0.1539	0.0076	3.1154

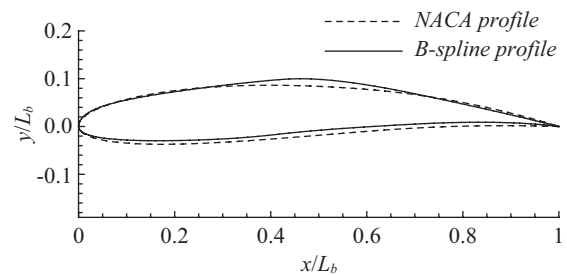


Fig. 13. Comparison of the optimal profiles.

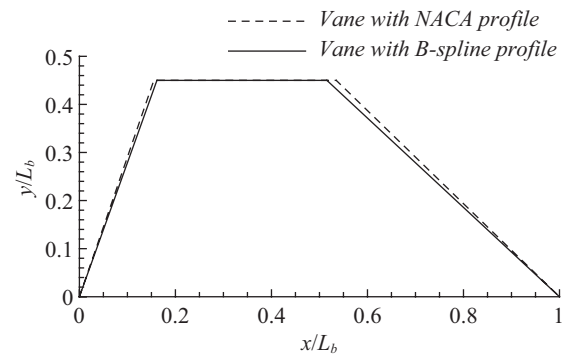


Fig. 14. Comparison of the optimal outlines.

than the NACA vane. On the other hand, the optimal NACA vane has a more streamlined profile than the B-spline vane, which consequently increases the lift of the NACA vane.

VII. CONCLUSIONS

The results show that the optimization procedure developed herein, which is based on a Genetic Algorithm, is a viable procedure for design of submerged vanes. Two types of methodology for vane shape construction are purposed, one is based on the NACA wing section and the other one is by B-splines. The final designs and their performances, measured in terms of lift, drag, and objective function value, are quite different. The design developed from the NACA profile has slightly higher lift and drag than that developed from the B-spline profile. So, if drag is a significant concern in a given project, the latter should probably be selected. If

drag were not a concern, the design developed from the NACA profile would give better performance. For overall considerations, the design with B-spline profile surpasses the other one. Both profiles show better performance comparing to conventional NACA profiles based on the objective function values. The results indicate that the procedure developed in this paper based on a Genetic Algorithm is robust in designing the submerged vanes. By taking advantage of the fast evolving computer technology, restriction on CPU time is no longer a major concern in flow calculations, and the favorable results suggest further explorations of submerged vane designs by using Genetic Algorithms in the future.

REFERENCES

1. Abbott, I. H. and von Doenhoff, A. E., *Theory of Wing Sections: Including a Summary of Airfoil Data*, Dover, New York, pp. 408-413 (1959).
2. Arora, J. S., *Introduction to Optimum Design*, McGraw-Hill, New York, pp. 20-23 (1989).
3. De Jong, K. A., *An Analysis of the Behavior of a Class of Genetic Adaptive Systems*, Ph.D. Dissertation, University of Michigan, Ann Arbor, MI (1975).
4. Goldberg, D. E., *Genetic Algorithms in Search, Optimization, and Machine Learning*, Addison-Wesley, Reading, MA, pp. 62-80 (1989).
5. Jameson, E., *Optimum Design Methods in Aerodynamics*, AGARD-VKI Lecture Series, Von Karman Institute, Belgium, pp. 124-132 (1994).
6. Katz, J. and Plotkin, A., *Low-Speed Aerodynamics*, McGraw-Hill, New York, pp. 102-108 (1991).
7. Odgaard, A. J. and Lee, H. Y. E., *Submerged Vanes for Flow Control and Bank Protection in Streams*, IIHR Report No. 279, Iowa Institute of Hydraulic Research, Iowa City, Iowa (1984).
8. Odgaard, A. J. and Mosconi, C. E., "Streambank protection by submerged vanes," *Journal of Hydraulic Engineering, ASCE*, Vol. 113, No. 4, pp. 520-536 (1987).
9. Odgaard, A. J. and Spoljaric, A., "Sediment control by submerged vanes," *Journal of Hydraulic Engineering, ASCE*, Vol. 112, No.12, pp. 1164-1181 (1986).
10. Odgaard, A. J. and Wang, Y., "Sediment management with submerged vanes. I: Theory," *Journal of Hydraulic Engineering, ASCE*, Vol. 117, No. 3, pp. 263-283 (1991).
11. Ouyang, H. T., "Investigation on the Dimension and shape of a submerged vane for sediment management in alluvial channels," *Journal of Hydraulic Engineering, ASCE*, Vol. 135, No. 3, pp. 209-217 (2009).
12. Ouyang, H. T., Weber, L., and Odgaard, A. J., "Design optimization of a two-dimensional hydrofoil by applying a genetic algorithm," *Engineering Optimization*, Vol. 38, No. 5, pp. 529-540 (2006).
13. Wang, Y. and Odgaard, A. J., "Flow control with vorticity," *Journal of Hydraulic Research*, Vol. 31, No. 4, pp. 549-562 (1993).